Research on Cross Regulation Rate Control Based on Equivalent Leakage Inductance Constraint of Flyback Multiwinding Transformer

Shaoliang An, *Member, IEEE*, Qing Wu, Hang Wang, *Student Member, IEEE*, Boyan Wang, and Fan Yang

***Abstract*—This article proposes a cross-regulation rate control method based on equivalent leakage inductance constraint of multiwinding transformer, to solve the problem of other output voltages seriously deviating from their rated values caused by changes in one load of Flyback converters. A detailed analysis is conducted on the distribution characteristics of leakage inductance in multiwinding transformers, revealing its inherent connection with the output voltage cross-regulation problem. The mathematical relationship that can accurately predict the cross-regulation rate through leakage inductance is derived, and the design principles for the leakage ratio of each winding in transformers are explained. A vector called magnetic field intensity area is defined to measure the leakage inductance value, and a multiwinding equivalent leakage inductance model that can be automatically solved is established. The optimal winding arrangement that takes into the requirements of low primary leakage inductance and proportional secondary leakage inductance is selected. An experimental prototype of a 30 W six output Flyback converter is built, and the cross-regulation rate is tested to be as low as 5%. The correctness and feasibility of the proposed multiwinding equivalent leakage inductance model and cross-regulation rate control method are verified.**

***Index Terms*—Cross-regulation rate control, equivalent leakage inductance model, multiwinding planar transformer.**

I. Introduction

THE multioutput Flyback converter can provide multiple different levels and isolated dc power supply voltages for power electronic devices and is widely used in military, aerospace, industry, civilian, and other fields. However, in actuality, the multiwinding transformer that plays the role of isolation and energy transfer in the converter cannot be fully coupled, and the coupling degree between each winding may not be the same. The load of each winding rarely changes synchronously, which leads to cross-regulation problems between the output voltages, and in severe cases, it can even affect the stable operation of the converter. Therefore, many scholars have conducted in-depth research on this issue.

In terms of parasitic parameter suppression in multiwinding transformers, Zhao et al. [1], Wu et al. [2], and Nayak and S. Nath [3] compared the influence of the interleaving degree of the primary and secondary windings on the flux distribution of the transformer and obtained the optimal winding arrangement method that balances equivalent series resistance and leakage inductance, providing new ideas for the multiwinding transformers design. However, the range of staggered types examined is limited, and the analysis becomes significantly more challenging when there are more than four outputs, as each one needs to be analyzed individually. Equivalent model of leakage inductance for three-terminal coupled inductors, which can contribute to the design of transformers with inductance characteristics in Flyback converters, is analyzed in [4] and [5]. A method of placing an unclosed copper strip as shielding around the winding conductors of the transformer to reduce leakage inductance is proposed in [6]. Leakage flux will induce eddy currents in the copper shielding, thereby reducing the amount of leakage flux and leakage inductance. But the method is not sufficient to completely alleviate the voltage spikes caused by leakage inductance in the circuit and may reduce the conversion efficiency. Ouyang et al. [7] proposed to decompose the leakage flux into two parts, longitudinal and transverse, in response to the traditional leakage inductance analysis method. A calculation formula for accurately solving the leakage inductance of planar transformers is derived. But the method is only suitable for cases where the ac magnetic flux is substantially parallel to the surface of rectangular conductors. Liu et al. [8] discussed the problem of mutual decoupling between windings, placing unrelated windings in the same core vertically and decoupling them using geometric characteristics to eliminate cross effects between corresponding output circuits.

In terms of control strategy optimization of multioutput Flyback converter, Sarkar et al. [9], [10] proposed a decoupling control method for an independent multioutput Flyback converter, which eliminates the cross-coupling relationship between control and output variables. But the additional switching devices make control more complex. Wang et al. [11] and Zhang et al. [12] proposed a model predictive voltage control method for multioutput dc–dc converters. Through an augmented state-space model, the output voltage ripple is predicted and

Received 23 July 2024; revised 12 November 2024; accepted 7 December 2024. Date of publication 16 December 2024; date of current version 28 January 2025. This work was supported by the National Natural Science Foundation of China under Grant 52207207. Recommended for publication by Associate Editor M. Ponce-Silva. *(Corresponding author: Shaoliang An.)*

Shaoliang An, Qing Wu, Hang Wang, and Boyan Wang are with the Department of Electrical Engineering, Xi'an University of Technology, Xi'an 710048, China (e-mail: shaoliang.an@xaut.edu.cn; 2211920003@stu.xaut.edu.cn; 1241910010@stu.xaut.edu.cn; 2231921116@stu.xaut.edu.cn).

Fan Yang is with the College of Automation and Artificial Intelligence, Nanjing University of Posts and Telecommunications, Nanjing 210023, China (e-mail: yangfan@njupt.edu.cn).

Color versions of one or more figures in this article are available at https://doi.org/10.1109/TPEL.2024.3518582.

Digital Object Identifier 10.1109/TPEL.2024.3518582

controlled, improving the cross-regulation performance of the converter. Charge-balanced current mode control and fixed frequency pulse width modulation for single-inductor dual-output boost converter, achieving minimal cross regulation in simulation, providing a new solution to the cross-regulation problem, but lacking experimental verification, were adopted in [13]. Tran and Choi [14] delved into the time division multiple control method for multioutput scenarios, which corresponds to a simple and reliable loop structure that can provide strict and uniform regulation for all outputs. Moreover, the voltage and current of each output need to be sensed for the time-division control. The weighted feedback method, which determines the proportion of a certain signal in the total feedback signal based on the voltage amplitude, so that each output is directly feedback regulated, which can significantly improve the accuracy of each output voltage, is analyzed in [15], [16], and [17]. However, its external circuit can easily reduce the power density of the converter.

In terms of circuit structure, Nayak and Nath [3] and Sanchis-Kilders et al. [18] proposed to series connect small value inductors outside each winding of the transformer according to the square ratio of turns, indirectly improving the accuracy of each output voltage. The volume of added inductors resulted in lower power density. Yang et al. [19], Satyaraddi et al. [20], and Kuruva et al. [21] proposed setting a linear voltage regulator on the output of the converter. This method is simple to implement and has high accuracy, but its power loss and volume cannot be ignored. Ahmad et al. [22] analyzed the working principle of magnetic amplifiers. When the output current is too large and the flux density exceeds a reasonable range, the magnetic amplifier can act as a switch to accurately control the output voltage in real time. However, the magnetic amplifier materials are expensive. Liu et al. [23] replaced the input/output inductors in two-port dc–dc converters with coupling inductors and used independent switches in the magnetic coupling branch, which mitigate the cross-regulation problem of conventional dual-output converters.

In terms of control schemes of leakage inductance, Sharma and Kimball [24] proposed a transformer with leakage and magnetizing inductance that can be independently adjusted by changing the air gap between the magnetic core legs to adjust the magnetizing inductance and changing the overlap area between the primary and secondary windings to adjust the leakage inductance. But this means that a larger core window area is required to adjust the area of winding overlap. Without sacrificing the core window utilization and power density of transformer, Xiao et al. [25] proposed an optimization method to minimize leakage inductance based on winding arrangement adjustment. In this method, the primary and secondary windings are rearranged in the same layer, and the magnetomotive force of the layer is minimized by a certain interleaved structure, so as to minimize the leakage inductance. But only the case of single-layer hybrid winding is discussed. The application of multilayer winding is further discussed in [26], and the leakage inductance is improved by adjusting the number of turns of each layer winding and the distance from the upper boundary of the window. For the asymmetric power flow problem of triple-active bridge converter, in order to obtain the desired phase-shift of terminal voltages at nominal power flow, a design method of asymmetric leakage is proposed by analyzing the relationship between power, phase-shift, and leakage inductance [27]. It is difficult to design electrical insulation for fully interleaved structures under high-voltage applications, Zhao et al. [28] proposed a method in which the primary winding is divided into two parts working in parallel, which can reduce leakage inductance and is suitable for high voltage applications. However, the increase of primary windings and insulation layers leads to a more complex design. For resonant converters, a matrix transformer is integrated with an adjustable resonant inductor in a five-leg core structure by rearranging the center-tap secondary windings, but only for the center-tap secondary windings [29]. Due to the need to utilize the leakage inductance of the coupling inductance to suppress electromagnetic interference on the ac side, Zhang and Jiang [30] proposed a coupled inductor structure for parallel inverters to increase the leakage inductance. This structure adds two additional magnetic rods on both sides of the U-shaped core to provide a low reluctance path for the leakage flux, thereby increasing the leakage inductance.

The above references mainly improved the cross-regulation performance of converters by adding components or optimizing control strategies, at the expense of the efficiency and power density of multioutput power supply to varying degrees. On the basis of the above research, this article deeply analyzes the circuit and magnetic source factors that cause cross regulation problems in converters. With the premise of not losing power conversion efficiency, a cross-regulation rate control method based on equivalent leakage inductance constraint of multiwinding planar transformers is proposed to fundamentally improve the cross-regulation performance of multioutput converters. Section II takes the six output Flyback converter as an example to analyze the influence of leakage inductance distribution in each winding of the transformer on the cross-regulation performance in detail. The relationship between the cross-regulation rate and the leakage inductance ratio of each winding is derived, and a specific method to improve the cross-regulation performance is explained. The role and importance of optimizing the leakage inductance distribution in improving this indicator are summarized. Section III delves into the numerical relationship between leakage inductance, magnetic field intensity, and core window energy, and establishes a multiwinding equivalent leakage inductance model that can be automatically solved. Based on this, the principle and steps of cross-regulation rate control are analyzed in detail. In Section IV, the correctness and feasibility of the multiwinding equivalent leakage inductance model, and cross-regulation rate control method are verified through experiments.

II. Multioutput Flyback Cross Regulation Problem

Cross-regulation problem refers to the phenomenon in a multioutput converter where a load change in one channel causes a drastic change in the output voltage of other channels. This section takes the six output Flyback converter as an example to analyze in detail the mechanism of this problem, derive the mathematical relationship between cross cross-regulation rate

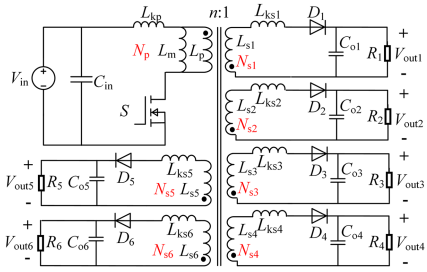

Fig. 1. Structure diagram of six-output Flyback.

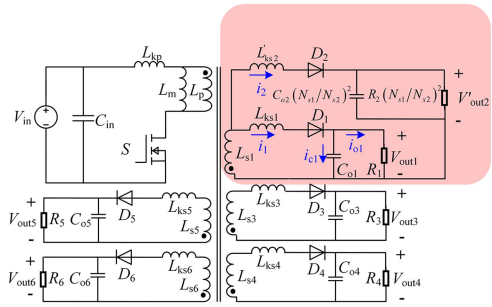

Fig. 2. Equivalent structure diagram of six output Flyback.

and leakage inductance of the transformer, and provide relevant measures to improve the cross-regulation performance.

A. Inherent Mechanism of Cross Regulation Problem

The structure of the six-output Flyback converter is shown in Fig. 1.

In Fig. 1, $L_{\rm p}$ is the primary inductance of the transformer, $L_{\rm m}$ is the primary excitation inductance, and $L_{\rm s1}$, $L_{\rm s2}$, $L_{\rm s3}$, $L_{\rm s4}$, $L_{\rm s5,}$ and $L_{\rm s6}$ are the secondary inductances of the first to sixth output windings. The turns of each winding on the primary and secondary sides are $N_{\rm p}$, $N_{\rm s1}$, $N_{\rm s2}$, $N_{\rm s3}$, $N_{\rm s4}$, $N_{\rm s5}$, and $N_{\rm s6}$, respectively. $L_{\rm kp}$ is the primary leakage inductance. $L_{\rm ks1}$, $L_{\rm ks2}$, $L_{\rm ks3}$, $L_{\rm ks4}$, $L_{\rm ks5,}$ and $L_{\rm ks6}$ are the leakage inductances of the first to sixth secondary winding. S is the primary switch. D_1, D_2, D_3, D_4, D_5, and D_6 are the secondary diodes. $C_{\rm in}$ is the input capacitor. $C_{\rm o1}$, $C_{\rm o2}$, $C_{\rm o3}$, $C_{\rm o4}$, $C_{\rm o5}$, and $C_{\rm o6}$ are the output capacitors. R_1, R_2, R_3, R_4, $R_{5,}$ and R_6 are the load resistances of the first to sixth output channel. $V_{\rm in}$ is the input voltage of the converter, $V_{\rm out1}$, $V_{\rm out2}$, $V_{\rm out3}$, $V_{\rm out4}$, $V_{\rm out5,}$ and $V_{\rm out6}$ are the output voltages of the first to sixth output channel in sequence.

Among the six outputs, only the output voltage $V_{\rm out1}$ corresponding to the secondary winding $N_{\rm s1}$ of the transformer participates in signal feedback. The output voltage accuracy and dynamic regulation performance are adjusted to the optimal state that meets the requirements, while the other output voltages are closed-loop regulated through the coupling relationship between windings. The output accuracy and anti-interference ability are insufficient, and the output voltage of the other windings are easy to rise or fall seriously when the load of winding $N_{\rm s1}$ is switched. Taking windings $N_{\rm s1}$ and $N_{\rm s2}$ as examples, analyze the variation characteristic of each output voltage.

Assuming that the leakage inductance of winding $N_{\rm s1}$ and winding $N_{\rm s2}$ in Fig. 1 satisfies

$$L_{\rm ks2} = xL_{\rm ks1} \tag{1}$$

where $L_{\rm ks1}$ is the leakage inductance of winding $N_{\rm s1}$ and $L_{\rm ks2}$ is the leakage inductance of winding $N_{\rm s2}$.Thus, x is the ratio coefficient of $L_{\rm ks1}$–$L_{\rm ks2}$.

To visually compare the relative changes between $V_{\rm out1}$ and $V_{\rm out2}$, the channel parameters corresponding to the primary winding $N_{\rm p}$ and the secondary winding $N_{\rm s1}$ are kept unchanged. The channel parameters corresponding to the $N_{\rm s2}$ are converted to the $N_{\rm s1}$ side, as shown in the red-shaded area in Fig. 2.

In Fig. 2, i_1 and i_2 are the leakage currents flowing through $L_{\rm ks1}$ and $L'_{\rm ks2}$, respectively. $i_{\rm o1}$ is the output current flowing through R_1, and $i_{\rm c1}$ is the charging current of $C_{\rm o1}$. According to the proportional relationship between inductance and turns, the leakage inductance $L'_{\rm ks2}$ can be expressed as

$$L'_{\rm ks2} = xL_{\rm s1}\left(\frac{N_{\rm s1}}{N_{\rm s2}}\right)^2. \tag{2}$$

In the ideal case, the forward voltage drops of D_1 and D_2 are equal. The parameters of winding $N_{\rm s2}$ are converted to winding $N_{\rm s1}$ so that the output voltage $V'_{\rm out2}$ after conversion is equal to $V_{\rm out1}$. When the transformer transfers energy to the secondary side, according to Kirchhoff's laws, the voltage of leakage inductor $L_{\rm ks1}$ on loop $L_{\rm s1}$-$L_{\rm ks1}$-D_1-$V_{\rm out1}$ and the voltage of leakage inductor $L'_{\rm ks2}$ on loop $L_{\rm s1}$-$L'_{\rm ks2}$-D_2-$V'_{\rm out2}$, and the voltage at both ends of $L_{\rm ks1}$ and $L'_{\rm ks2}$ can be expressed as $V_{\rm k}$

$$V_{\rm k} = V_{\rm s} - V_{\rm D} - V_{\rm out1} = V_{\rm s} - V_{\rm D} - V'_{\rm out2}. \tag{3}$$

Taking S turn off as the initial time, the currents i_1 and i_2 at time t can be derived

$$\begin{cases} i_1 = \int_0^t \frac{V_{\rm k}}{L_{\rm ks1}}{\rm d}\tau = \frac{V_{\rm k}}{L_{\rm ks1}}t \\ i_2 = \int_0^t \frac{V_{\rm k}}{L_{\rm ks2}\left(\frac{N_{\rm s1}}{N_{\rm s2}}\right)^2}{\rm d}\tau = \frac{V_{\rm k}}{xL_{\rm ks1}\left(\frac{N_{\rm s1}}{N_{\rm s2}}\right)^2}t \end{cases}. \tag{4}$$

The proportional relationship between two leakage currents can be obtained

$$k_i = \frac{i_2}{i_1} = \frac{1}{x}\left(\frac{N_{\rm s2}}{N_{\rm s1}}\right)^2. \tag{5}$$

In (5), k_i is the ratio between two leakage currents.

Plot the curve of k_i changing with x, as shown in Fig. 3.

Analyzing Fig. 3, when $x<(N_{\rm s2}/N_{\rm s1})^2$, the leakage current i_2 of $N_{\rm s2}$ that does not participate in feedback is greater than i_1 of $N_{\rm s1}$. Therefore, when i_1 reaches the sum of its required output current $i_{\rm o1}$ and charging current $i_{\rm c1}$, the energy transfer of the transformer ends, and i_2 has already exceeded the rated value at the same time, causing the output voltage $V_{\rm out2}$ without feedback regulation to overshoot during dynamic adjustment or exceed its rated level during steady-state operation. When $x>(N_{\rm s2}/N_{\rm s1})^2$, the variation law of i_2 that does not participate in feedback is opposite.

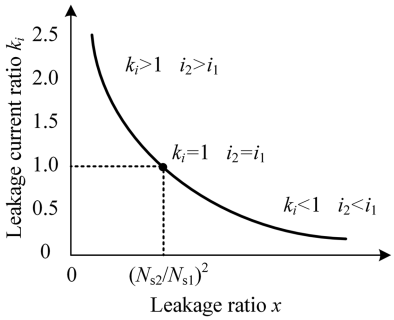

Fig. 3. Variation curve of current ratio k_i with leakage ratio x.

B. Cross Regulation Rate

The indicator for measuring the impact of cross regulation on the output voltage of a converter is the cross-regulation rate, which refers to the ratio of the maximum output voltage variation to the rated value of ith channel when a certain load changes in a multioutput converter. Its definition formula is

$$S_{\text{outi}} = \frac{U_{i1} - U_{i2}}{U_{i\_N}} \times 100\%. \tag{6}$$

In (6), U_{i1}, U_{i2}, and $U_{\text{i\_N}}$ are the maximum, minimum, and rated output voltage of ith channel, respectively.

However, (6) can only reflect the basic definition of cross-regulation rate and cannot reflect the inherent relationship between the indicator and the distribution of leakage inductance in each winding. In order to accurately predict its value based on electrical parameters during system design, it is necessary to derive the determining formula of cross-regulation rate from the root cause.

In n-output converters, only one output voltage participates in signal feedback, and the corresponding leakage current is i_{FB}. The leakage currents of the other nonfeedback windings are $i_{\text{no\_FB1}}$, $i_{\text{no\_FB2}}$, …, $i_{\text{no\_FBn}}$, respectively. $L_{\text{k\_FB}}$, $L_{\text{k\_noFB1}}$, $L_{\text{k\_noFB2}}$, …, $L_{\text{k\_noFBn}}$ are the leakage of the secondary feedback winding and nonfeedback windings of the transformer, and N_{FB}, $N_{\text{no\_FB1}}$, $N_{\text{no\_FB2}}$, …, $N_{\text{no\_FBn}}$ correspond to their winding turns. R_{FB}, $R_{\text{no\_FB1}}$, $R_{\text{no\_FB2}}$, …, $R_{\text{no\_FBn}}$ correspond to their load resistance. V_{FB}, $V_{\text{no\_FB1}}$, $V_{\text{no\_FB2}}$, …, $V_{\text{no\_FBn}}$ correspond to their actual output voltage. $V_{\text{FB\_N}}$, $V_{\text{no\_FB1\_N}}$, $V_{\text{no\_FB2\_N}}$, …, $V_{\text{no\_FBn\_N}}$ correspond to their rated output voltage. P_{FB}, $P_{\text{no\_FB1}}$, $P_{\text{no\_FB2}}$, …, $P_{\text{no\_FBn}}$ correspond to their rated output power.

If the rated output power and rated output voltage of both feedback winding N_{FB} and nonfeedback winding $N_{\text{no\_FBi}}$ satisfy the relationship equation

$$P_{\text{no\_FBi}} = a_{\text{i}} P_{\text{FB}},\ V_{\text{no\_FBi\_N}} = k_{\text{i}} V_{\text{FB\_N}}. \tag{7}$$

In (7), a_{i}, k_{i} are constant coefficients.

According to (5) and combining Ohm's law, the proportional relationship between the output voltage of the N_{FB} and $N_{\text{no\_FBi}}$ can be obtained under actual condition

$$\frac{V_{\text{no\_FBi}}}{V_{\text{FB}}} = k_{\text{i}} \frac{L_{\text{k\_FB}}}{L_{\text{k\_noFBi}}} \left(\frac{N_{\text{noFBi}}}{N_{\text{FB}}} \right)^2. \tag{8}$$

Considering that the output voltage V_{FB} participates in feedback, it is approximately assumed that the output voltage of this channel is equal to its rated value

$$V_{\text{FB}} = V_{\text{FB\_N}}. \tag{9}$$

By combining (7), (8), and (9), the proportional relationship between the actual and rated output voltage of each nonfeedback winding can be obtained

$$\frac{V_{\text{no\_FBi}}}{V_{\text{no\_FBi\_N}}} = \frac{L_{\text{k\_FB}}}{L_{\text{k\_noFBi}}} \left(\frac{N_{\text{noFBi}}}{N_{\text{FB}}} \right)^2. \tag{10}$$

No matter how the load resistance and output power of each channel change, the formula shown in (10) always holds. Therefore, when the load of the feedback channel suddenly changes, the output voltage change of each nonfeedback channel is determined by the leakage ratio of the feedback winding to the nonfeedback winding.

Furthermore, the determining formula for the cross-regulation rate of the ith output voltage can be obtained

$$S_{\text{outi}} = \left| 1 - \frac{L_{\text{k\_FB}}}{L_{\text{k\_noFBi}}} \left(\frac{N_{\text{no\_FBi}}}{N_{\text{FB}}} \right)^2 \right| \times 100\%. \tag{11}$$

Observing (11), it can be seen that when the turns ratio of the transformer winding is determined, the factor that affects the cross-regulation rate is only the leakage inductance ratio between the feedback and each nonfeedback winding and is independent of the load condition of the converter.

If $(L_{\text{k\_FB}}/L_{\text{k\_noFB}}) > (N_{\text{no\_FB}}/N_{\text{FB}})^2$, the feedback channel switches from full to light load, the output voltage of the nonfeedback channel easily overshoot.

If $(L_{\text{k\_FB}}/L_{\text{k\_noFB}}) = (N_{\text{no\_FB}}/N_{\text{FB}})^2$, when the converter takes places any load-switching action, the nonfeedback output voltage changes are consistent with the feedback channel.

If $(L_{\text{k\_FB}}/L_{\text{k\_noFB}}) < (N_{\text{no\_FB}}/N_{\text{FB}})^2$, the feedback channel switches from full to light load, the output voltage of the nonfeedback channel easily drops.

At the same time, the closer the cross-regulation rate is to 1, the stronger the cross regulation ability of the converter, and the higher the output voltage accuracy. The fundamental measure to improve this indicator is to allocate the leakage inductance of each secondary winding as much as possible according to the square ratio of turns. Due to the reliance on manual production, traditional wounded transformers have obvious process errors, making it difficult to accurately predict and control the distribution of leakage inductance in each winding. Therefore, planar transformers with parasitic parameters that can be accurately calculated have more advantages.

III. Equivalent Leakage Inductance Model and Cross Regulation Rate Control Method

After clarifying the optimization method for cross-regulation rate, the arrangement of windings becomes crucial. Starting from the distribution of leakage in each winding of the transformer, this section analyzes in detail the numerical relationship between leakage inductance, core window energy, and magnetic field intensity integration. An equivalent leakage inductance model

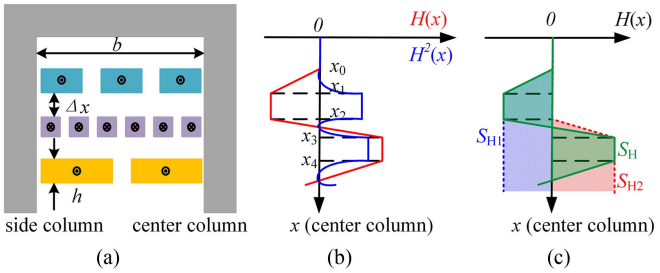

Fig. 4. Diagram for calculating the primary leakage. (a) 1/2 core window. (b) Magnetic field intensity. (c) Intensity area.

for multiwinding transformers is established, and based on leakage inductance constraints, a cross-regulation rate control method that takes into account the efficiency of the transformer is proposed. Using MATLAB, the optimal winding arrangement meets the requirements of low primary leakage inductance and the proportional secondary leakage inductance.

A. Equivalent Mathematical Relationship Between Leakage Inductance and Magnetic Field Intensity

The precondition for accurately controlling the leakage ratio of each winding is to clarify the calculation method of the leakage inductance value, which provides a theoretical basis for quantitative control of leakage inductance. Therefore, taking the primary leakage inductance as an example, the mathematical relationship is derived.

The primary leakage inductance essentially refers to the inductance corresponding to the flux leaked to the outside of the core when the transformer's primary flux is not fully coupled to the secondary, and the energy stored in this part of the flux mostly exists in the core window. Therefore, the value of the primary leakage inductance can be calculated by quantifying the energy stored in the window. Fig. 4 shows the zoom in locally on the left half of the EI core window.

Fig. 4 uses the center column as the vertical axis with a starting point from the top position of the window, and makes the distance x (from each position of the window to the top) as an independent variable. According to Ampere's loop theorem, the magnetic field intensity $H(x)$ at position x can be calculated and its curve can be drawn, and the calculation formula for the primary leakage inductance can be obtained

$$L_{\mathrm{kp}} = \frac{\mu_0 bc \sum_{i=1}^{4} \int_{x_{i-1}}^{x_i} H_i(x)^2 dx}{I_{\mathrm{p}}^2}. \tag{12}$$

Observing (12), due to μ_0, b, c, and I_{p} are all constants, the value of primary leakage inductance is essentially determined by the integration of $H^2(x)$ in the x direction. Draw the curve of $H^2(x)$ changing with x, as shown in the blue part of Fig. 4(b). The larger the surrounding area between $H^2(x)$ and the x-axis, the greater the primary leakage inductance. Due to the fact that the area of the blue part is equal to the parabolic integral, direct calculation is complex, and the computational complexity needs to be simplified while ensuring accuracy. By analyzing the numerical relationship between $H^2(x)$ and the $H(x)$, it can be concluded that the integration of the two curves in the x-axis direction is positively correlated. Therefore, the larger the area enclosed by the $H(x)$ curve and the x-axis, the greater the value of the primary leakage inductance. The primary leakage inductance can be equivalently measured by the area enclosed by the $H(x)$ and x-axis.

B. Multiwinding Equivalent Leakage Model

After realizing the determining factor of leakage inductance, it becomes crucial to calculate the area enclosed by $H(x)$ and the x-axis. Considering that there are many winding arrangements for multioutput transformers, and different arrangement orders correspond to different $H(x)$ curves and leakage inductance distributions. According to the principle of arrangements and combinations, there are $m!$ orders for m-layer windings. When $m \geq 5$, it is very difficult to manually select the optimal solution according to the above calculation method for various arrangements. Therefore, it is necessary to establish a multiwinding equivalent leakage inductance model that can be solved automatically by computer.

First, define the vector: magnetic field intensity area S_{H}, which is used to characterize the influence degree of the ampere-turns carried by a certain winding on the accumulated energy inside the window, as shown in the blue area in Fig. 4(c).

If the jth winding with $N_{\mathrm{j}}I_{\mathrm{j}}$ is arranged from the initial position of the x-axis, then the ampere-turn of the first winding is N_1I_1, and the magnetic field intensity generated by it increases linearly in the axial direction of the PCB area in that layer. Therefore, the effective length of the effect of N_1I_1 on the magnetic field intensity area $S_{\mathrm{H1\_h}}$ in the first layer of PCB is $h/2$. If the distance $\triangle x$ between the first and second layers is also divided into the range of the first layer PCB, then within the $\triangle x$ region, the magnetic field intensity generated by N_1I_1 has risen to its maximum value and remains unchanged. Therefore, the effective length of its influence on $S_{\mathrm{H1\_}\triangle x}$ in the region is $\triangle x$.

The expression for the total magnetic field intensity area generated by N_1I_1 within the window can be written as

$$S_{H1} = \left(\frac{h}{2} + \Delta x\right) N_1I_1 + (h + \Delta x) N_1I_1 + \cdots + (h + \Delta x) N_1I_1. \tag{13}$$

Similarly, the magnetic field intensity area generated by the N_2I_2 arranged on the second layer PCB in the window is shown in the red area of Fig. 4(b), and its expression is

$$S_{H2} = \left(\frac{h}{2} + \Delta x\right) N_2I_2 + (h + \Delta x) N_2I_2 + \cdots + (h + \Delta x) N_2I_2. \tag{14}$$

Add the S_{Hj} generated by each $N_{\mathrm{j}}I_{\mathrm{j}}$ within the window, and the algebraic sum obtained is the area $S_{\mathrm{H\_1\&2}}$ enclosed by the entire window magnetic field intensity $H(x)$ and the x-axis

$$S_{H\_1\&2} = S_{H1} + S_{H2} = \begin{bmatrix} N_1I_1 & N_2I_2 \end{bmatrix} \begin{bmatrix} \frac{h}{2} + \Delta x & h + \Delta x \\ 0 & \frac{h}{2} + \Delta x \end{bmatrix}. \tag{15}$$

When there are m-layer windings, the total magnetic field intensity area $S_{\mathrm{H\_all}}$ is expressed in matrix product form, which is the multiwinding equivalent leakage inductance model

$$S_{H\_\mathrm{all}} = \begin{bmatrix} N_1 I_1 \\ N_2 I_2 \\ \vdots \\ N_m I_m \end{bmatrix}^T \begin{bmatrix} \left(\frac{h}{2} + \Delta x\right) + (m-1)(h + \Delta x) \\ \left(\frac{h}{2} + \Delta x\right) + (m-2)(h + \Delta x) \\ \vdots \\ \left(\frac{h}{2} + \Delta x\right) + (m-m)(h + \Delta x) \end{bmatrix} = \lambda \cdot K. \quad (16)$$

The $S_{\mathrm{H\_all}}$ shown in (16) is the area enclosed by the $H(x)$ curve and the x-axis as shown in Fig. 4(c). Although this value is not equal to the actual leakage energy, it can be used to effectively measure the magnitude of the primary leakage inductance. The right coefficient matrix K is determined by the thickness of the PCB winding layer and the distance between layers and does not change with the arrangement. Therefore, by simply changing the elements order of the array λ on the left, solving for $S_{\mathrm{H\_all}}$ under all arrangements and sorting them, the array λ that meets the requirements of the leakage inductance and the corresponding optimal winding arrangement can be found.

C. Cross Regulation Rate Control Method

According to the above analysis, the fundamental measure to improve the cross-regulation rate is to allocate the secondary leakages according to the square ratio of turns. However, the number of multiwinding arrangements is huge, and the winding arrangement that meets the requirements of secondary leakage distribution may not be able to achieve the minimum primary leakage inductance, resulting in a significant loss in the energy transfer process of the transformer. In response to this issue, this article proposes a cross-regulation rate control method based on the optimization results of the core mentioned above and the equivalent leakage inductance model of multiwinding. The aim is to flexibly control the element order of the array λ, screen out the corresponding winding arrangement, and maximize the satisfaction of the primary and secondary leakage inductance index requirements. While distributing the secondary leakage inductance according to the square ratio of the turns, the primary leakage inductance is minimized. There is no need to increase the energy transfer loss of the transformer for achieving precise control and optimization of cross-regulation rate.

First, multiwinding arrangements with low primary leakage inductance are selected using MATLAB to narrow the range of secondary selection. Then, calculate the secondary leakage inductance corresponding to each arrangement by the magnetic field energy method shown in (11). Calculate the weighted variance s^2 of the secondary leakage inductance by taking the square ratio of each turn to the total secondary winding turns as the weight

$$s^2 = \sum_{j=1}^{6} \left(\left(\frac{N_{sj}}{N_{s\Sigma}}\right)^2 L_{ksj} - \frac{1}{6} \sum_{j=1}^{6} \left(\frac{N_{\mathrm{sj}}}{N_{s\Sigma}}\right)^2 L_{\mathrm{ksj}} \right)^2. \quad (17)$$

The smaller the weighted variance s^2 shown in (17), the more uniform the coupling degree of each secondary winding, and the corresponding cross-regulation rate is also smaller. Therefore, within the range of secondary selection, select the array λ with the smallest s^2, which is the optimal winding arrangement order. This method can accurately predict and optimize the cross-regulation rate without compromising the primary leakage inductance index of the transformer, achieving a balanced improvement in the efficiency and cross-regulation performance of the multioutput converter.

TABLE I
DESIGN INDICATORS OF A 30 W SIX OUTPUT FLYBACK CONVERTER

Parameter	Value
Input voltage range V_{in}	110–240 VAC
output voltage $V_{\mathrm{out1}}/V_{\mathrm{out2}}/V_{\mathrm{out3}}/V_{\mathrm{out4}}/V_{\mathrm{out5}}/V_{\mathrm{out6}}$	24/+12/-12/5/18/18V
Cross regulation rate S_{out2} ,S_{out3} ,S_{out4} ,S_{out5} ,S_{out6}	33%,33%,6.7%,30%,38%
Primary inductance L_{p}	213.5 μH
Coupling coefficient of primary and secondary	>0.99
Turns ratio N_{p}: N_{s1}: N_{s2}: N_{s3}: N_{s4}: N_{s5}: N_{s6}	24 :4 :2 :2 :1 :3 :3

TABLE II
CALCULATION RESULTS OF L^{KP} AND s^2 OF 5 WINDING ARRANGEMENT STRUCTURES

	Structure 1	Structure 2	Structure 3	Structure 4	Structure 5
L_{kp}/uH	0.21	0.18	0.17	0.18	0.18
s^2	0.008	0.0033	0.0033	0.0052	0.0052

IV. SIMULATION AND EXPERIMENT

To verify the application effect of the cross-regulation rate control method mentioned above in multioutput Flyback converters, as well as the correctness of the multiwinding equivalent leakage inductance model supporting this method, an experimental prototype is constructed for a 30 W six-output Flyback transformer to verify the above method.

The design indicators of the converter are shown in Table I.

Due to the fact that there are seven windings, and the number of turns on the primary winding is relatively high ($N_{\mathrm{p}} = 24$), if all of them are wound on one layer of PCB, it will cause the window area to be too large, which will have a negative effect on the power density of the transformer. Therefore, it is chosen to wind 24 turns of primary winding on 4 layers of PCB, while 6 secondary windings are wound on separate 6 layers of PCB, totaling 10 layers to be arranged. In order to improve the efficiency of transformer and cross-regulation characteristics of the multioutput converter, primary leakage inductance and weighted variance of secondary leakage should be reduced. According to the equivalent leakage inductance model in Section III, five winding structures with smaller primary leakage inductance are obtained. Based on the above cross-regulation rate control method and combined with the indicators shown in Table I, the weighted variances of the secondary leakage inductance of five winding arrangement structures are calculated in Table II.

Finally, Structure 3 with the smallest value of both L_{kp} and s^2 is selected, as shown in Fig. 5.

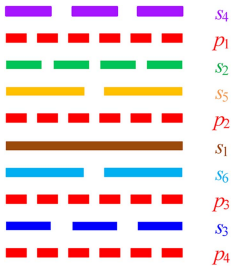

Fig. 5. Optimal winding arrangement scheme.

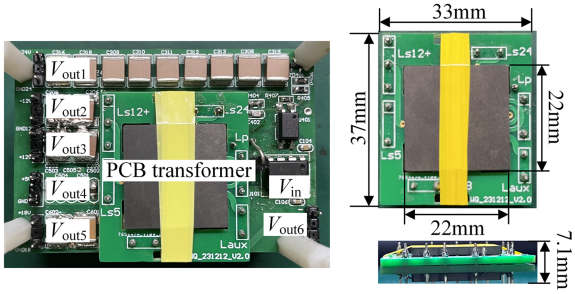

Fig. 6. Thirty watts six-output Flyback experimental platform. (a) Thirty watts six-output Flyback converter. (b) PCB transformer with X-core.

TABLE III
MEASURED VALUES OF SELF INDUCTANCE AND LEAKAGE INDUCTANCE OF EACH WINDINGS

winding	L_m/uH	L_k/uH	L_{ks1}/L_{ksi}	Value range
N_p	212.9	0.526	-	-
N_{s1}	6.173	0.114	-	-
N_{s2}	1.543	0.039	2.9	[2.95.2]
N_{s3}	1.569	0.038	3.0	[2.95.2]
N_{s4}	0.402	0.007	15.2	[15.217.0]
N_{s5}	3.483	0.056	2.05	[0.53.0]
N_{s6}	3.432	0.064	1.77	[1.22.3]

Building an experimental prototype according to the above design result, where the output voltages V_{out1}, V_{out2}, V_{out3}, V_{out4}, V_{out5}, and V_{out6} correspond to the transformer windings L_{s1}, L_{s2}, L_{s3}, L_{s4}, L_{s5}, and L_{s6} shown in Fig. 1, respectively, and only the V_{out1} participates in feedback, as shown in Fig. 6. The height of the transformer in Fig. 6 is only 7.1 mm, covering an area of 1221 mm^2, and the power density is 56.71 W/in^3.

A. Primary and Secondary Leakage Test

According to (11), the range of leakage inductance ratio between the feedback winding and each nonfeedback winding is calculated, and the self-inductance and leakage inductance data of each winding of the transformer is measured, as shown in Table III. The value range in the last column of Table III represents the range of leakage inductance ratio, i.e., L_{ks1}/L_{ks2}.

Table III shows that the coupling coefficient of the primary and secondary sides of the transformer is 0.9971, and the leakage inductance ratio of each nonfeedback winding and feedback winding on the secondary side is within the required range of the cross-regulation rate. This indicates that the selected arrangement method takes into account the efficiency and cross-regulation rate of the transformer, and the solution method of equivalent leakage inductance model is feasible.

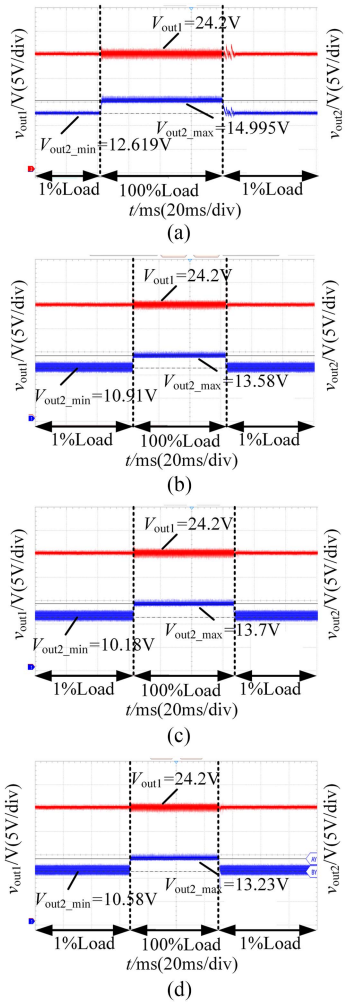

Fig. 7. Output voltage of N_{s1} under different load conditions when switching the N_{s2} load. (a) Winding N_{s2} output 10% load. (b) Winding N_{s2} output 50% load. (c) Winding N_{s2} output 75% load. (d) Winding N_{s2} output 100% load.

B. Cross Regulation Rate Test

To verify the load capacity and dynamic regulation of each output of the converter, the input voltage $V_{in} = 100$ V is maintained, and the load of feedback winding N_{s1} is switched between 100% and 10%, respectively, when the nonfeedback winding N_{s2} outputs 10%, 50%, 75%, and 100% load. Test the changes in V_{out1} and V_{out2}, and all other windings remain 100% loaded, as shown in Fig. 7(a)–(d).

Analyzing the voltage waveform shown in Fig. 7(a), the output voltage corresponding to feedback winding N_{s1} always maintains $V_{out1} = 24.2$ V throughout the load switching process, with output accuracy $\sigma_1 = 0.083\%$, meeting the indicator requirements, with a small steady-state error of the system. When switching load, the overshoot values of the two output voltages are $\sigma_{out1} = 1.1\%$, $\sigma_{out2} = 5.0\%$, and the setting time is $t_s = 3.7$ ms, indicating good dynamic regulation performance.

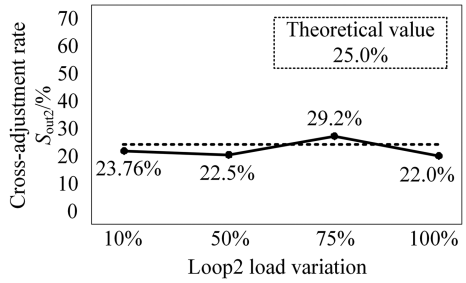

Fig. 8. Line graph of cross-regulation rate under different load in N_{s2}.

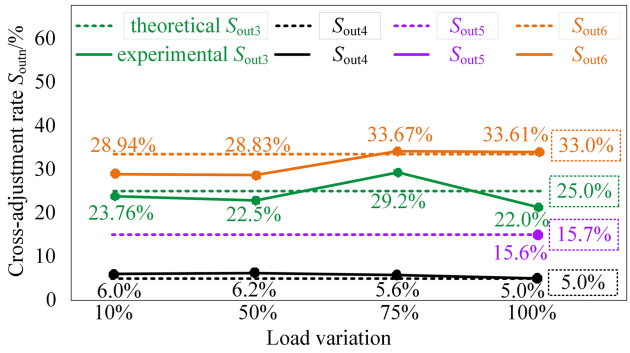

Fig. 9. Cross-regulation rate curves of all outputs.

According to waveforms in Fig. 7(b)–(d), under 50%, 75%, and 100% load, the cross-regulation rates of the output voltage corresponding to N_{s2} are $S_{out2\_50\%} = 22.5\%$, $S_{out2\_75\%} = 29.2\%$, $S_{out2\_100\%} = 22.0\%$, all meet the requirements of the indicators. According to the determination formula for the cross-regulation rate shown in (11), the theoretical cross-regulation rate for V_{out2} is calculated as follows:

$$S'_{out2} = \left|1 - \frac{L_{ks1}}{L_{ks2}}\left(\frac{N_{s2}}{N_{s1}}\right)^2\right| \times 100\% = 25\%. \quad (18)$$

Measured values of the cross-regulation rate of V_{out2} are summarized under different load, and curve is plotted as shown in Fig. 8.

Observing Fig. 8, it can be seen that under different loads, the cross-regulation rate of the V_{out2} remains basically unchanged and is close to the theoretical calculation value. Due to the presence of other stray parameters in the channel besides leakage inductance, and the uneven forward voltage drop of each secondary diode, both can affect the steady-state accuracy and dynamic performance of the converter. Therefore, there is an error of no more than 4.2% between the experimental results and the theoretical value. The experimental results show that the cross regulation of the six-output converter is only determined by the leakage ratio of each winding, and is independent of the system operating conditions. Moreover, the derived cross-regulation rate determination formula can accurately predict this indicator, which has strong accuracy and feasibility.

Similarly, test the actual cross-regulation rates of output voltages V_{out1}, V_{out2}, V_{out3}, V_{out4}, V_{out5}, and V_{out6} under different load conditions, and theoretically calculate them according to (11). All other nonfeedback windings are maintained at 100% load whenever testing a nonfeedback winding, meaning only the loads of the test channel and feedback loop are altered. Cross-regulation rate curves of each output voltage are drawn under different operating conditions, as shown in Fig. 9.

The test can only be conducted under full load conditions since V_{out5} is dedicated to supplying power to the auxiliary power control chip, thereby limiting the flexibility of load switching. Observing Fig. 9, it can be seen that for each output voltage, the cross-regulation rate does not change significantly with the change of load conditions and is close to the theoretical calculation value. This verifies the conclusion that the cross-regulation performance is only determined by the distribution of leakage inductance in each winding of the transformer and

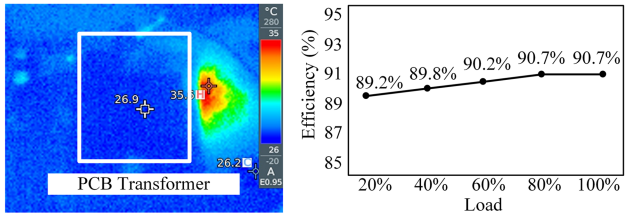

Fig. 10. Heat generation and efficiency of the converter. (a) Temperature rise at full load. (b) Efficiency curve over the full load range.

also supports the accuracy of the derived cross-regulation rate determination formula. The cross-regulation rate of the five output voltages meets and is superior to the indicators, and the cross-regulation rate of V_{out4} can be as low as 5.0% under 100% load conditions. This verifies the correctness and feasibility of the cross-regulation rate control method based on the equivalent leakage inductance constraint mentioned above.

C. Efficiency and Heat Dissipation Characteristics Test

The above experimental results can ensure that the transformer corresponding to the 30 W experimental platform meets the requirements of output voltage and load capacity. To compare and verify the heat dissipation performance of the transformer, no external heat sink is added. The prototype is tested under ambient temperature of 25 °C, minimum input voltage $V_{in} = 100$ V, and output power $P_{out} = 30$ W (full load). At this time, the current flowing through the primary winding of the transformer is the highest. After the circuit operates stably for 20 min and the temperature rise of each component is stable, the operating temperature of the transformer is recorded, as shown in Fig. 10(a).

In Fig. 10(a), under the working condition of ambient temperature of 25 °C and full load, the operating temperature rise of the PCB transformer is only 1.9 °C, indicating good heat dissipation performance. This indirectly indicates that the flux density distribution inside the core is uniform, and there is no current crowding phenomenon in the winding. The minimum input voltage is maintained at $V_{in} = 100$ V, the efficiency of the converter is measured at 20%, 40%, 60%, 80%, and 100% load, and the efficiency curve is plotted as shown in Fig. 10(b). It can be seen that the transformer operates under light load conditions,

TABLE IV
COMPARISON TO STATE OF THE ART

Reference	[9]	[30]	This Work
Topology	Flyback	Flyback	Flyback
Input voltage	48 VDC	120 VDC	110–240 VAC
Output voltage	15/5V	21/27/33V	24/+12/-12/5/18/18V
Output power	40 W	16.2 W	30 W
Number of outputs	2	3	6
Peak efficiency	88.22%	83.5%	90.7%

with an efficiency of 89.2%. As the load increases, the maximum efficiency of the entire machine at full load can reach 90.7%. Considering that active clamping and synchronous rectification structures are not used in the design, the overall efficiency of the transformer can still be maintained at a high level even with high switching frequency and rectifier diode conduction loss.

The experimental results show that without adding inductors, linear regulators, and weighted optocoupler feedback links, arranging the transformer windings according to the proposed cross-regulation rate control method can significantly improve the cross-regulation performance of the multioutput converter. Considering the fact that the calculation conditions of leakage energy are not affected by the working conditions of the transformer, the proposed method is suitable for transformers in various power electronic topologies and has strong practicality and universality.

A comparison of this work and other multioutput converters is summarized in Table IV. For low-power converters, the efficiency is generally not high [9], [31], and some inherent losses such as device losses in the circuit often account for a large proportion of total power, making it difficult to improve the efficiency numerically. In addition, multiwinding means more secondary devices, which is also a challenge for improving efficiency. Compared with the references in Table IV, this article has the minimum power and the most windings. This work has the highest efficiency and shows the effectiveness of the proposed method.

V. CONCLUSION

This article conducts in-depth research on the cross-regulation problem of multioutput Flyback converters. Through the numerical relationship of leakage current between each channel, it is clear that the problem is caused by the inconsistent coupling degree of each winding of the transformer. The fundamental method to optimize the cross-regulation rate is to design the secondary leakage of the transformer according to the square ratio of turns. The theoretical calculation formula derived can accurately predict the cross-regulation rate of each output voltage of the transformer. The conclusion that the integral of the magnetic field intensity in the core window is directly proportional to the leakage inductance is obtained through mathematical deduction. A multiwinding equivalent leakage inductance model that can be automatically solved is established, and a cross-regulation rate control method is proposed based on this. Then, a winding arrangement that meets the requirements of low primary leakage and proportional secondary leakage is selected. The experimental results of 30-W six output Flyback converter show that the cross-regulation rate control method proposed in this article can effectively improve the cross-regulation performance of multioutput converters without sacrificing efficiency, and achieve a balanced improvement of system efficiency and cross-regulation characteristics. At the same time, the equivalent leakage inductance model and the cross-regulation rate control method can be extended to various types of multioutput power electronic converters, which have good feasibility and universality.

REFERENCES

[1] B. Zhao, Z. Ouyang, M. A. E. Anderson, M. Duffy, and W. G. Hurley, "An improved partially interleaved transformer structure for high-voltage high-frequency multiple-output applications," in *Proc. 43rd Annu. Conf. IEEE Ind. Electron. Soc.*, 2017, pp. 798–804.

[2] X. Wu, H. Chen, and Z. Qian, "1-MHz LLC resonant DC transformer (DCX) with regulating capability," *IEEE Trans. Ind. Electron.*, vol. 63, no. 5, pp. 2904–2912, May 2016.

[3] G. Nayak and S. Nath, "Small signal modeling and analysis of single input three output buck converter using coupled inductor," in *Proc. Nat. Power Electron. Conf.*, 2019, pp. 1–6.

[4] Y. Guan, X. Hu, S. Zhang, Y. Wang, D. Xu, and W. Wang, "A low profile high frequency LED driving system based on aircore planar inductor," in *Proc. nt. Power Electron. Conf.*, 2018, pp. 614–618.

[5] Y. Guan, Y. Cheng, T. Yao, Y. Wang, W. Wang, and D. Xu, "Analysis and design of a step-up converter based on three-end planar coupled inductor," in *Proc. IEEE Ind. Appl. Soc. Ann. Meeting*, 2021, pp. 1–7.

[6] T. Strous and G. Simonelli, "Improved power transformer performance using leakage inductance shielding," in *Proc. Eur. Space Power Conf.*, 2019, pp. 1–6.

[7] Z. Ouyang, W. G. Hurley, and M. A. E. Andersen, "Improved analysis and modeling of leakage inductance for planar transformers," *IEEE Trans. Emerg. Sel. Topics Power Electron.*, vol. 7, no. 4, pp. 2225–2231, Dec. 2019.

[8] Y. Liu, O. Ziwei, and M. A. E. Andersen, "Integrated inductors design for GaN-based ZVS bridgeless single-SEPIC PFC," in *Proc. IEEE 12th Energy Convers. Congr. Expo. -Asia*, 2021, pp. 1625–1631.

[9] A. Sarkar, N. Deshmukh, and S. Anand, "Modified PWM scheme to reduce reverse conduction loss in GaN-based independently controlled multiple output flyback converter," *IEEE Trans. Power Electron.*, vol. 37, no. 11, pp. 12968–12972, Nov. 2022.

[10] A. Sarkar, B. T. Vankayalapati, and S. Anand, "GaN-based multiple output flyback converter with independently controlled outputs," *IEEE Trans. Ind. Electron.*, vol. 69, no. 3, pp. 2565–2576, Mar. 2022.

[11] B. Wang, V. R. K. Kanamarlapudi, L. Xian, X. Peng, K. T. Tan, and P. L. So, "Model predictive voltage control for single-inductor multiple-output DC–DC converter with reduced cross regulation," *IEEE Trans. Ind. Electron.*, vol. 63, no. 7, pp. 4187–4197, Jul. 2016.

[12] X. Zhang, B. Wang, X. Tan, H. B. Gooi, H. H.-C. Iu, and T. Fernando, "Deadbeat control for single-inductor multiple-output DC–DC converter with effectively reduced cross regulation," *IEEE J. Emerg. Sel. Topics Power Electron.*, vol. 8, no. 4, pp. 3372–3381, Dec. 2020.

[13] H. A V, P. Patra, M. Parmar, and N. Chen, "Cumulative charge balanced single-inductor dual-output converter for improved transient and cross regulation," in *Proc. IEEE Appl. Power Electron. Conf. Expo.*, 2024, pp. 712–718.

[14] V.-L. Tran and W. Choi, "Novel time division multiple control method for multiple output battery charger," *IEEE Trans. Power Electron.*, vol. 29, no. 10, pp. 5102–5105, Oct. 2014.

[15] D. Astolfi and L. Praly, "Integral action in output feedback for multi-input multi-output nonlinear systems," *IEEE Trans. Autom. Control*, vol. 62, no. 4, pp. 1559–1574, Apr. 2017.

[16] D. E. Koshy and S. T K, "Design and analysis of a power factor corrected quad output off-line isolated AC to DC universal power supply with improved cross-regulation," in *Proc. IEEE Int. Conf. Power Electron., Drives Energy Syst.*, 2022, pp. 1–6.

[17] N. Tang, M. Yang, K. Hu, and D. Xu, "Research on state feedback of two-mass system based on weight coefficient," in *Proc. IEEE Transp. Electrific. Conf. Expo, Asia–Pac.*, 2017, pp. 1–6.
[18] E. Sanchis-Kilders et al., "Stability improvement of isolated multiple-output DC/DC converter using coupled inductors," *IEEE Trans. Aerosp. Electron. Syst.*, vol. 52, no. 4, pp. 1644–1653, Aug. 2016.
[19] S.-H. Yang et al., "A single-inductor dual-output converter with linear amplifier-driven cross regulation for prioritized energy-distribution control of envelope-tracking supply modulator," in *Proc. IEEE Int. Solid-State Circuits Conf.*, Feb. 2017, pp. 36–37.
[20] C. G. Satyaraddi, A. Usha, A. Bhat, P. K. Praveen, B. K. Singh, and V. Chippalktti, "Design and implementation of multiple output interleaved flyback converter with post regulators," in *Proc. IEEE Int. Conf. Elect., Comput. Commun. Technol.*, Feb. 2019, pp. 1–6.
[21] S. Kuruva, C. G. Satyaraddi, K. E. Rayees, B. K. Singh, and V. Chippalkatti, "Design and implementation of multiple output DC-DC converter with output power sequencing," in *Proc. 6th Int. Conf. Convergence Technol.*, 2021, pp. 1–7.
[22] S. S. Ahmad, A. Raj, and G. Narayanan, "Improved direct-coupled high-bandwidth voltage amplifier for B-H characterization of magnetic materials," in *Proc. IEEE Int. Conf. Power Electron., Drives Energy Syst.*, 2022, pp. 1–6.
[23] Y. Liu, G. Chen, Y. Hu, L. Huang, and X. Qing, "Magnetic coupling branch based dual-input/output DC–DC converters with improved cross-regulation and soft-switching operation," *IEEE Trans. Ind. Electron.*, vol. 67, no. 9, pp. 7167–7178, Sep. 2020.
[24] A. Sharma and J. W. Kimball, "Novel transformer with variable leakage and magnetizing inductances," in *Proc. 2021 IEEE Energy Convers. Congr. Expo.*, 2021, pp. 2155–2161.
[25] X. Guo, C. Li, Z. Zheng, and Y. Li, "General analytical model and optimization for leakage inductances of medium-frequency transformers," *IEEE J. Emerg. Sel. Topics Power Electron.*, vol. 10, no. 4, pp. 3511–3524, Aug. 2022.
[26] Y. Xiao, X. Guo, C. Li, and Z. Zheng, "A leakage inductance adjustment model of hybrid winding arrangement medium frequency transformer," in *Proc. IEEE Energy Convers. Congr. Expo.*, 2023, pp. 5677–5683.
[27] D.-U. Kim, S. Kim, B.-J. Byeon, and B. H. Jeong, "Design of asymmetric inductance for multi-port active bridge converter," in *Proc. 2022 IEEE Energy Convers. Congr. Expo.*, 2022, pp. 1–6.
[28] B. Zhao, G. Wang, W. G. Hurley, and Z. Ouyang, "An interleaved structure for a high-voltage planar transformer for a travelling-wave tube," in *Proc. IEEE 8th Int. Power Electron. Motion Control Conf.*, 2016, pp. 3695–3701.
[29] A. Nabih, Q. Li, and F. C. Lee, "Magnetic integration of four-transformer matrix with high controllable leakage inductance using a five-leg magnetic," in *Proc. IEEE Appl. Power Electron. Conf. Expo.*, 2022, pp. 693–700.
[30] Y. Zhang and D. Jiang, "A new coupled inductor structure with larger leakage inductance for EMI suppression," in *Proc. IEEE 10th Int. Symp. Power Electron. Distrib. Gener. Syst.*, 2019, pp. 51–54.
[31] R. Wang and J. Zhang, "A simple current balancing method for multi-output flyback LED driver," in *Proc. IEEE 2nd Int. Future Energy Electron. Conf.*, 2015, pp. 1–5.

Shaoliang An (Member, IEEE) received the B.S., M.S., and Ph.D. degrees in electrical engineering from the Xi'an University of Technology, Xi'an, China, in 2005, 2010 and 2014, respectively.

From 2017 to 2019, he was a Postdoctoral Researcher with the Center for Power Electronics Systems, Virginia Polytechnic Institute and State University, Blacksburg, VA, USA. Since 2005, he has been with the Xi'an University of Technology, and is currently an Associate Professor with the Department of Electrical Engineering. His research interests include high-frequency power conversion, modeling and control of power converters, and renewable energy systems.

Qing Wu received the B.S. and the M.S. degrees in electrical engineering from the Xi'an University of Technology, Xi'an, China, in 2021 and 2024, respectively.

Her research interests include the design of multi-output flyback converters and high-frequency planar magnetic integration techniques.

Hang Wang (Student Member, IEEE) received the B.S. and the M.S. degrees in electrical engineering from the Xi'an University of Technology, Xi'an, China, in 2021 and 2024, respectively, where he is currently working toward the Ph.D. degree in electrical engineering.

His main research interests include magnetic integration and resonant converters.

Boyan Wang received the B.S. degree in electrical engineering and automation from the Shaanxi University of Science and Technology, Xi'an, China, in 2023. He is currently working toward the M.S. degree in electrical engineering from the Xi'an University of Technology, Xi'an.

His current research interests include topology of dc–dc converters and high frequency planar magnetic integration technologies.

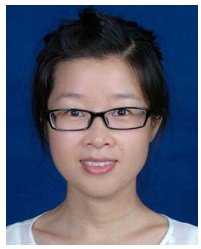

Fan Yang was born in Shanxi, China, in 1985. She received the B.S. degree in electrical engineering from Nanjing Normal University, Nanjing, China, in 2007, and the M.S. and Ph.D. degrees in electrical engineering from the Nanjing University of Aeronautics and Astronautics, Nanjing, in 2013 and 2020, respectively.

She is currently an Associate Professor with the College of Automation and Artificial Intelligence, Nanjing University of Posts and Telecommunications, Nanjing, China. Her research interests include topology and control of dc–dc and dc–ac converters.